Supporting Information

Wang et al. 10.1073/pnas.1411694111

SI Text

Fig. S1: Test for α-Syn Binding/Colocalization with Organelles. We asked whether α-synuclein (α-syn) binds or colocalizes with mitochondria, lipid droplets, or peroxisomes. Mitochondria were imaged using the plasmid-born reporter Dld2–GFP (Dld2, mitochondrial D-lactate dehydrogenase) (1), and two strains were constructed to image lipid droplets or peroxisomes in *psd1*Δ cells. (The plasmid bearing Dld2–GFP was a gift from Zhengchang Liu, University of New Orleans, New Orleans, Louisiana.) In one strain, *ERG6*–red fluorescent protein (RFP) replaced the genomic copy of *ERG6* (see ref. 2), whereas in the other strain, *PEX3–RFP* replaced the genomic copy of *PEX3*—these strains are called *psd1*Δ–ERG6–RFP and *psd1*Δ–PEX3–RFP, respectively. Erg6 is a resident lipid droplet protein (3). Pex3 is required for peroxisome biogenesis (4). GFP and RFP are the GFPs and RFPs, respectively.

To test for the binding of α-syn to mitochondria, cells transformed with α-syn–RFP and Dld2–GFP plasmids were grown in synthetic complete (SC) mixed medium at 30 °C, and after 5.5 h, the fluorescence images were taken. In wild-type cells, mitochondria appeared as long, green tubular structures, whereas the red α-syn molecules localized to the perimeter of the cells (Fig. S1*A*, *Top*). In *psd1*Δ cells without ethanolamine (ETA), mitochondria formed clusters of green puncta, whereas red α-syn appeared as a large cytoplasmic focus, which we attribute to the endoplasmic reticulum (ER) (Fig. S1*A*, *Middle*). No appreciable overlap occurred between α-syn and the fragmented mitochondria. Incubation of *psd1*Δ cells with ETA did not change the fragmented nature of the mitochondria; however, ETA redistributed α-syn from the ER to the plasma membrane (Fig. S1*A*, *Bottom*).

We previously reported that α-syn–GFP binds to lipid droplets in wild-type cells when the cells are cultured in medium supplemented with oleate (2). Furthermore, the binding of α-syn to lipid droplets is sensitive to the composition of phospholipids in the cells, which is medium-dependent. To test for the binding of α-syn to lipid droplets in *psd1*Δ cells cultured in mixed medium [1% sucrose (Suc)/1% galactose (Gal)], *psd1*Δ*–ERG6–RFP* cells transformed with plasmid pAG426–α-syn–GFP were induced for 5 h and then imaged using fluorescence microscopy. In most cells, α-syn–GFP clustered in several large, bright green cytoplasmic foci (Fig. S1*B*, *Left*). Many cells also contained lipid droplets, which appeared as smaller red foci (Fig. S1*B*, *Center*). In general, α-syn–GFP foci and the lipid droplets do not overlap; instead, the two bodies appear to be in close proximity to each other (Fig. S1*B*, *Right*). A close spatial association between these two bodies is not surprising given that α-syn–GFP is retained in the ER (Fig. 2*A*) and lipid droplets originate from ER membranes.

To test for the binding of α-syn to peroxisomes, *psd1*Δ*–PEX3–RFP* cells transformed with plasmid pAG426–α-syn–GFP were induced for 5 h and then imaged using fluorescence microscopy (2). No overlap was found between peroxisomes (Pex3–RFP) and α-syn–GFP foci (Fig. S1*C*). On the basis of these experiments, we conclude that the α-syn–GFP foci in *psd1*Δ cells are not due to the association of α-syn–GFP with mitochondria, lipid droplets, or peroxisomes.

Fig. S2: Test Whether ETA Dissolves Preformed α-syn–GFP Foci. We asked whether ETA could dissolve preformed α-syn–GFP foci and whether ETA could rescue the severe growth defect that occurs in *psd1*Δ cells that express α-syn. First, to see whether ETA could dissolve preformed α-syn–GFP foci, ETA (5 mM) was added at 0, 3, or 6 h after the start of induction in mixed medium, and images were taken after 7 h of induction. ETA dissolved most of the preformed α-syn–GFP foci (Fig. S2*A*). Second, we analyzed growth in liquid medium under two conditions—that is, 1% Suc/1% Gal (mix) or 2% (wt/vol) Gal. For the mixed medium (Fig. S2*B*), adding ETA at 5.5 h resulted in a reproducible increase in the growth rate. A much more dramatic effect was observed for *psd1*Δ cells cultured in the 2% Gal medium, which gives higher α-syn expression. When ETA was added after a 28.5-h induction, at which time there is a severe growth defect, there is a rapid growth burst, and the rate of this burst almost matches that of cells that had ETA the entire time (Fig. S2*C*). Overall, these experiments show that ETA added to *psd1*Δ cells containing preformed α-syn–GFP foci reduces the number of α-syn–GFP foci in cells and rescues growth.

Fig. S3: Phospholipid analysis using TLC. A sample of lipid extract was separated on a TLC plate using solvent mixture B [chloroform:methanol:ammonium hydroxide (65:25:4)]. After being sprayed with 10% sulfuric acid, the plate was colorized in an oven at 120 °C. The developed plate was scanned and the intensities of the PE and PC bands were determined.

Fig. S4: Test for Respiratory Defects in *psd1*Δ Cells. O_2 consumption by wild-type and *psd1*Δ cells was measured with a Clark electrode (Fig. S4*A*). The rate of O_2 consumption by *psd1*Δ cells is ∼60% less than the rate of O_2 consumption by wild-type cells, which is consistent with an earlier study (5). Supplementing *psd1*Δ cells (± α-syn) with ETA failed to increase the rate of O_2 consumption. In wild-type cells (±α-syn), ETA slightly inhibited the rate of O_2 consumption. We also found that the complex III inhibitor antimycin A (AA), which induces respiratory stress, did not induce the formation of α-syn–GFP foci (Fig. S4*B*).

Fig. S5. Given that ETA prevents the formation of α-syn–GFP foci in *psd1*Δ cells, we tested whether ETA had the same effect on wild-type cells. For all of the experiments described below, cells were induced for 5 h in SC–Gal (2% Gal) dropout media. α-syn–GFP partitioned into large cytosolic foci in the wild-type cells (Fig. S5*A*), and ETA reduced the number of foci per cell as visualized using fluorescence microscopy, although the magnitude of the reduction was difficult to quantify. ETA treatment also abolished the band that we attribute to hyperphosphorylated α-syn (Fig. S5 *B* and *C*). Analysis of phospholipids chemically extracted from wild-type and *psd1*Δ cells revealed that ETA increased the level of phosphatidylethanolamine (PE) in wild-type cells (±α-syn) by 50–100% (Fig. S5*D*).

Fig. S6. Several BY4741 yeast deletion mutants (*fzo1*Δ, *fmp30*Δ, *spf1*Δ, and *atg8*Δ) (Open Biosystems) were tested for α-syn–GFP foci. *FZO1* encodes for mitofusin, which is involved in mitochondrial fusion (6). *FMP30* encodes for a mitochondrial protein involved in maintaining cardiolipin levels and mitochondrial morphology (7). *SPF1* encodes for a P-type ATPase that regulates Ca^{+2} homeostasis in the ER (8). *ATG8* encodes for a protein responsible for autophagosome biogenesis (9). α-syn–GFP failed to form foci in these mutants (Fig. S6).

Other. We found that low levels of PE trigger intense ER stress (Fig. 2 *B* and *D*) in *psd1*Δ cells, which was unaffected by moderate expression of α-syn, and ETA partially rescued this effect. Our interpretation of these results is that lipid disequilibrium in the ER causes this stress. Lipid disequilibrium in the ER has been previously linked to ER stress. For example, obesity leads to chronic

ER stress, and this may play a role in diabetes and insulin resistance. ER membranes isolated from obese mice contain more phosphatidylcholine (PC) than ER membranes from lean mice (10). The PC/PE ratio equals 2 for ER isolated from obese mice compared with 1.3 for lean mice. This lipid imbalance inhibits the sarco/ER calcium ATPase (10), and inhibition of this protein disrupts calcium homeostasis and triggers the unfolded protein response. Yeast express a similar P-type ATPase called Spf1 that regulates Ca^{+2} import into the ER (11). The amount of ER stress in *spf1*Δ cells was not much higher than that in wild type, and α-syn–GFP failed to form foci in this mutant (Fig. S6); therefore, ER stress caused by lipid disequilibrium in *psd1*Δ cells is probably not due to the inhibition of Spf1.

We found that α-syn forms foci in *ino2*Δ and *cho2*Δ even though these two mutants have normal levels of PE and no ER stress (Fig. 2 *C–E*). The level of PC is probably too low in these two mutants. We propose that a compensatory mechanism exists whereby PE functionally substitutes for PC in membranes when the level of PC is low. Furthermore, if PE substitutes for PC in the various cell membranes, then the PE level in the ER could decrease such that the transport of GPI-anchored proteins to the plasma membrane is partially blocked; in such a case, α-syn forms foci.

The *psd1*Δ mutant displayed intense cell wall stress (Fig. 4*B*), which indicates that low PE levels activate the cell wall integrity (CWI) pathway. Activation of this stress pathway leads to the rapid induction of the expression of a group of genes that code for proteins that serve to repair damage to the cell wall. We found that α-syn partially inhibits cell wall stress in *psd1*Δ cells (12), which means that the cells can only partially repair damage to the cell wall due to low PE levels (Fig. 4*B*). We therefore conclude that, in an environment dominated by ER stress induced by low levels of PE, *psd1*Δ cells expressing α-syn are likely to die from a combination of inhibition of the CWI pathway by α-syn and inefficient processing of GPI-anchored proteins.

Overall, we found that low cellular PE in *psd1*Δ cells produces defects in mitochondrial functions (inhibited respiration and fragmented mitochondria), which are not rescued by ETA, and in extramitochondrial functions (ER stress, vesicular trafficking defects, α-syn foci), which are rescued by ETA. Our results are consistent with added ETA restoring the level of PE in the ER via the Kennedy pathway, which partially rescues the observed defects in the extramitochondrial functions.

SI Materials and Methods

Plasmids. The plasmids used in this study are given in Table S1. Plasmid propagation and purification followed standard protocols (13). (*i*) Plasmids pAG426–α-syn–GFP and pAG426–α-syn–RFP were prepared using the in vitro recombination-based Gateway cloning system (Invitrogen) as described previously (12, 14). α-syn and GFP were PCR amplified from pAG426–α-syn and pTF301 (15). (*ii*) Plasmid pRS315–Fur4–EGFP was constructed as follows. FUR4 was amplified from genomic DNA (BY4741). The reverse primer contained a sequence complementary to the C-terminal FUR4 (about 25 nucleotides) and the N-terminal of EGFP (about 25 nucleotides). EGFP was amplified from pAG426–EGFP. The forward primer contained a sequence complementary to the C-terminal FUR4 (about 25 nucleotides) and the N-terminal of EGFP (about 25 nucleotides). These two PCR products were used as templates to amplify full-length FUR4–EGFP using primers containing SpeI and SacI sites. After digestion with the two restriction enzymes and purification, the fragment was ligated into pRS315 digested with the same enzymes. (*iii*) Plasmid pRS315–DsRed–HDEL (HDEL, the peptide histidine–aspartic acid–glutamic acid–leucine) was made by excising the NdeI–XbaI preKar2–DsRed–HDEL insert from plasmid YIPLac204TKC–DsRed–Express2–HDEL (Addgene) and then subcloning the insert into pET21a. After digestion of the resultant plasmid with HindIII–XbaI, the insert was subcloned into pRS315. (*iv*) Plasmid pMCZ-Y (16) was a gift from David Eide (University of Wisconsin–Madison, Madison, Wisconsin). Plasmid inserts were verified by sequencing at the Iowa State DNA Sequencing Facility.

Lipid Extraction. Total phospholipids were chemically extracted from yeast cells using the Folch et al. protocol (17). After 5 h of induction, 70 OD_{600} equivalents of cells were harvested, washed, and resuspended with 70 μL breaking buffer (20 mM Tris·Cl pH7.5, 1 mM EDTA, 1 mM DTT, and 1 mM PMSF). After adding 100 μL of glass beads, cells were vortexed for 5 min at 4 °C. After determining protein content, 70 μL of the lysate was transferred to a new microtube, to which 1.5 mL $CHCl_3$:MeOH (2:1,v:v) was added to extract the phospholipids. The tube was centrifuged at 15,000 × *g* for 5 min, and then 1 mL of the upper phase was transferred to a new tube. This crude lipid extract was washed (200 μL of deionized water), and after a brief centrifugation, the water phase was removed, and the interface was rinsed three times with 200 μL of MeOH:water (333:200, vol/vol). The remaining organic phase was dried, and the resulting film was dissolved in 50 μL of $CHCl_3$:MeOH (2:1, v:v); this is the phospholipid extract.

TLC. TLC was used to separate phospholipids extracted from yeast cells (18). We spotted 10 μL of the phospholipid extract per lane of the TLC (Silica gel plate 60, Merck). After air drying for 2 min, the plate was placed in the saturated chamber containing 107 mL of solvent mixture A [$CHCl_3$:ethanol: H_2O:triethylamine (30:35:7:35, v:v:v:v)] or solvent mixture B [chloroform:methanol:ammonium hydroxide (65:25:4)]. When the solvent front reached 1 cm from the top of the plate, the plate was removed and dried in a fume hood for 30 min. To visualize the phospholipids, the plate was sprayed with 10% sulfuric acid and baked in an oven at 120 °C until the phospholipid bands appeared. Phospholipid content of individual bands was determined as described below.

Phospholipid Quantification. ***Phosphate analysis (solvent mixture A).*** Phosphate was analyzed by the method of Zhou and Arthur (18). For a phosphate in individual bands, after a band was scraped off the TLC plate, it was transferred to an 11-mL glass tube, to which 0.3 mL concentrated perchloric acid was added. The tube was heated in an oven at 150 °C for 4 h to digest the lipids. We added 100 μL of this digest to 1 mL of a solution mix made up of three volumes of 0.4% malachite green in water, one volume of 4.2% ammonium molybdate (wt/vol) in 5 M HCl, and 0.125 volume of 1.5% Tween 20 (wt/vol) in water. After 20 min, the absorbance at 660 nm was measured. For the total phosphate, the phosphate in 10 μL of phospholipid extract was determined by the same method as described above. For any PE (or PC) band, its percentage is given by $[Pi]/[Pi]_{tot}$, where [Pi] is the concentration of phosphate in the digested PE band and $[Pi]_{tot}$ is the total phosphate in the sample before separation. This analysis was done for the data in Fig. 2*E*.
Band intensity analysis (solvent mixture B). After developing a TLC plate using the sulfuric acid treatment, as described above, the plate was scanned, and the mean intensity of individual bands was quantified using the Adobe Photoshop histogram function. For analysis of phospholipids from *psd1*Δ cells, the ratio of PE to PC (PE_s/PC_s) was determined, and the histogram in Fig. 1*E* uses the normalized ratio of $PE_s/PC_s/PE_{WT}/PC_{WT}$, where s and WT denote sample (with indicated treatment) and wild-type control cells (vector/–ETA).

Oxygen Consumption. The rate of O_2 consumption was measured at 30 °C using an YSI 5300 biological oxygen monitor (Yellow Springs Instrument) equipped with a Clark-type electrode. Yeast cells were grown to exponential phase in SC mixed medium at 30 °C. We added 3.2 mL of each culture to the chamber inserted with the Clark-type electrode. The chamber was sealed, and O_2 consumption was monitored over several minutes. The rate of consumption is reported in O_2%/min/10^7 cells.

1. Chelstowska A, Liu Z, Jia Y, Amberg D, Butow RA (1999) Signalling between mitochondria and the nucleus regulates the expression of a new D-lactate dehydrogenase activity in yeast. *Yeast* 15(13):1377–1391.
2. Wang S, et al. (2013) A peroxisome biogenesis deficiency prevents the binding of alpha-synuclein to lipid droplets in lipid-loaded yeast. *Biochem Biophys Res Commun* 438(2):452–456.
3. Binns D, et al. (2006) An intimate collaboration between peroxisomes and lipid bodies. *J Cell Biol* 173(5):719–731.
4. Hettema EH, Girzalsky W, van Den Berg M, Erdmann R, Distel B (2000) Saccharomyces cerevisiae pex3p and pex19p are required for proper localization and stability of peroxisomal membrane proteins. *EMBO J* 19(2):223–233.
5. Chan EY, McQuibban GA (2012) Phosphatidylserine decarboxylase 1 (Psd1) promotes mitochondrial fusion by regulating the biophysical properties of the mitochondrial membrane and alternative topogenesis of mitochondrial genome maintenance protein 1 (Mgm1). *J Biol Chem* 287(48):40131–40139.
6. Hermann GJ, et al. (1998) Mitochondrial fusion in yeast requires the transmembrane GTPase Fzo1p. *J Cell Biol* 143(2):359–373.
7. Kuroda T, et al. (2011) FMP30 is required for the maintenance of a normal cardiolipin level and mitochondrial morphology in the absence of mitochondrial phosphatidylethanolamine synthesis. *Mol Microbiol* 80(1):248–265.
8. Cronin SR, Rao R, Hampton RY (2002) Cod1p/Spf1p is a P-type ATPase involved in ER function and Ca2+ homeostasis. *J Cell Biol* 157(6):1017–1028.
9. Nakatogawa H, Ichimura Y, Ohsumi Y (2007) Atg8, a ubiquitin-like protein required for autophagosome formation, mediates membrane tethering and hemifusion. *Cell* 130(1):165–178.
10. Fu S, et al. (2011) Aberrant lipid metabolism disrupts calcium homeostasis causing liver endoplasmic reticulum stress in obesity. *Nature* 473(7348):528–531.
11. Cronin SR, Khoury A, Ferry DK, Hampton RY (2000) Regulation of HMG-CoA reductase degradation requires the P-type ATPase Cod1p/Spf1p. *J Cell Biol* 148(5):915–924.
12. Wang S, et al. (2012) α-Synuclein disrupts stress signaling by inhibiting polo-like kinase Cdc5/Plk2. *Proc Natl Acad Sci USA* 109(40):16119–16124.
13. Maniatis T, Fritsch EF, Sambrook J (1982) *Molecular Cloning: A Laboratory Manual* (Cold Spring Harbor Lab Press, Cold Spring Harbor, NY).
14. Lee YJ, Wang S, Slone SR, Yacoubian TA, Witt SN (2011) Defects in very long chain fatty acid synthesis enhance alpha-synuclein toxicity in a yeast model of Parkinson's disease. *PLoS ONE* 6(1):e15946.
15. Flower TR, Chesnokova LS, Froelich CA, Dixon C, Witt SN (2005) Heat shock prevents alpha-synuclein-induced apoptosis in a yeast model of Parkinson's disease. *J Mol Biol* 351(5):1081–1100.
16. Ellis CD, et al. (2004) Zinc and the Msc2 zinc transporter protein are required for endoplasmic reticulum function. *J Cell Biol* 166(3):325–335.
17. Folch J, Lees M, Sloane Stanley GH (1957) A simple method for the isolation and purification of total lipides from animal tissues. *J Biol Chem* 226(1):497–509.
18. Zhou X, Arthur G (1992) Improved procedures for the determination of lipid phosphorus by malachite green. *J Lipid Res* 33(8):1233–1236.

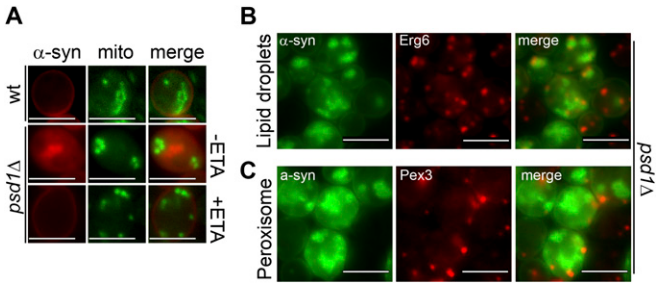

Fig. S1. α-syn does not colocalize with mitochondria, lipid droplets, or peroxisomes. (*A*) *psd1*Δ cells, transformed with plasmids pAG426–α-syn–RFP and pDLD2–GFP, were induced for 5 h (±ETA, 5 mM) in mixed medium and then imaged using fluorescence microscopy. (*B*) *psd1*Δ*–ERG6–RFP* cells, transformed with plasmid pAG426–α-syn–GFP, were induced for 5 h in mixed medium and then imaged. (*C*) *psd1*Δ*–PEX3–RFP* cells, transformed with plasmid pAG426–α-syn–GFP, were induced for 5 h in mixed medium and then imaged. The "merge" image is an overlay of the GFP and RFP images. (Scale bar, 5 μm.)

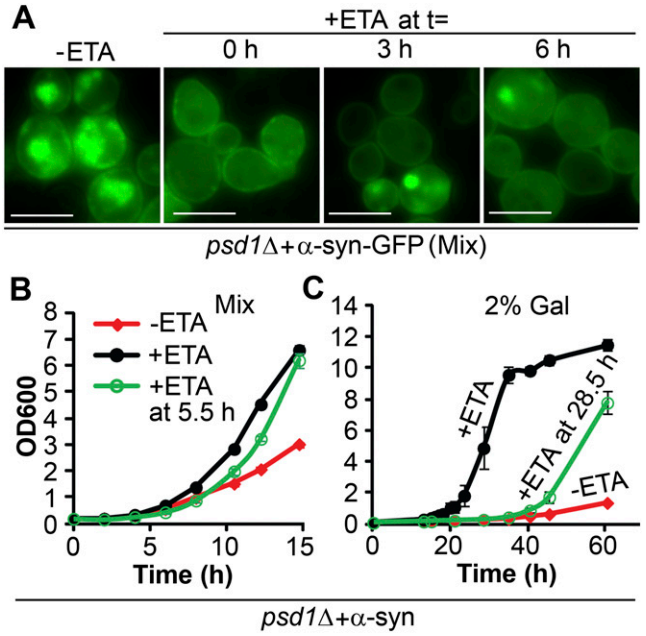

Fig. S2. ETA eliminates preformed cytoplasmic α-syn–GFP foci. (*A*) α-syn–GFP forms foci in *psd1*Δ cells. *psd1*Δ cells transformed with plasmid pAG426–α-syn–GFP were induced for 5 h in mixed medium (1% Suc/1% Gal) at 30 °C and then imaged by fluorescence microscopy. ETA (5 mM) was added upon transfer to inducing medium (t = 0), at 3 h or 6 h postinduction. (*B* and *C*) Growth curves of *psd1*Δ cells expressing α-syn (pAG426–α-syn) [mixed or 2% (wt/vol) Gal]. Points are the mean ± SD from three experiments.

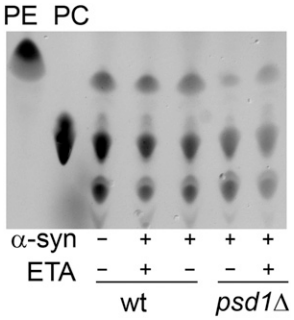

Fig. S3. Phospholipid analysis using TLC. Total lipids were extracted from the 50-μL cell lysate with CHCl3:methanol (2:1, vol/vol). The lipid sample was separated on a TLC plate using solvent mixture B [chloroform:methanol:ammonium hydroxide (65:25:4)]. After being sprayed with 10% sulfuric acid, the plate was colorized in an oven at 120 °C. The developed plate was then scanned and the intensities of the PE and PC bands were determined (*Materials and Methods*).

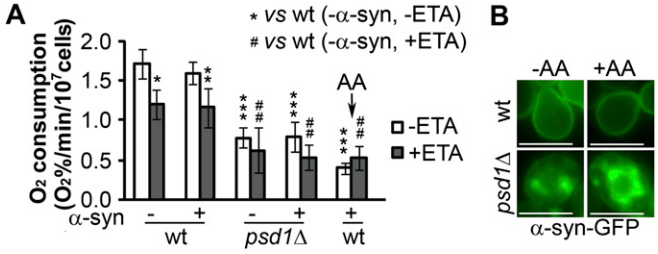

Fig. S4. Respiration is reduced in *psd1*Δ cells, and ETA fails to rescue the respiration defect. (*A*) O_2 consumption. See *Materials and Methods* for details. Values are mean ± SD ($n = 3$). $*^{\#}P < 0.05$, $**^{\#\#}P < 0.01$, and $***^{\#\#\#}P < 0.001$ using one-way ANOVA with Dunnet post hoc test. (*B*) AA does not induce α-syn–GFP foci. Fluorescence was obtained after a 5.5-h induction in SC mixed medium (± 15 μM AA).

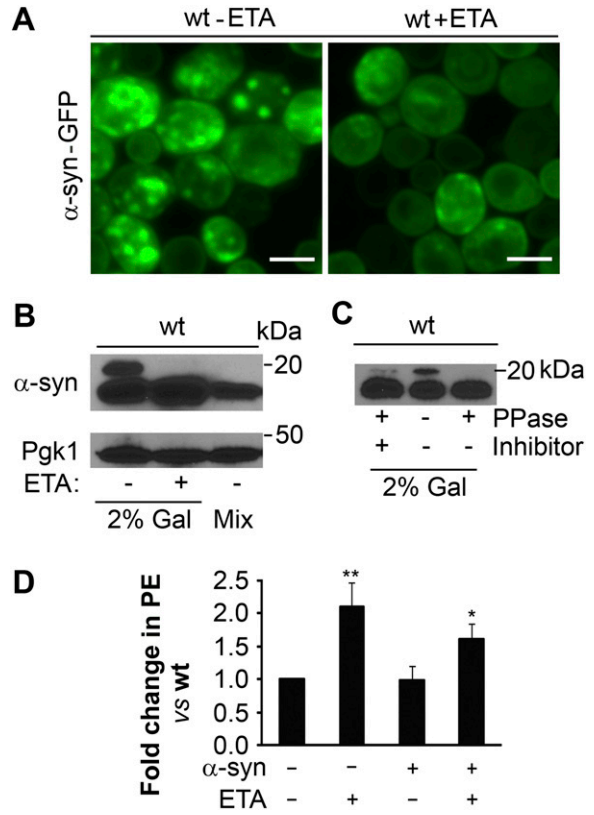

Fig. S5. α-syn foci formation and the effect of ETA on wild-type yeast cells. (*A*) α-syn–GFP forms foci in *psd1*Δ cells. Yeast cells transformed with the indicated plasmids were induced for 5 h in mixed medium (1% Suc/1% Gal) at 30 °C and then imaged using fluorescence microscopy. ETA (5 mM) was used for the rescue. (*B*) Western blotting of α-syn in wild-type cells. Lysates were prepared after a 5-h induction in 2% (wt/vol) Gal with or without 5 mM ETA or mixed media and then subjected to SDS/PAGE and Western blotting with an α-syn antibody. Pgk1 is a loading control. (*C*) Western blotting to analyze multiple phosphorylated α-syn. Lysate of wild-type cells was prepared after a 5-h induction in 2% Gal medium and treated with calf intestinal alkaline phosphatase (CIAP) or CIAP and its inhibitor for 1 h at 37 °C. The untreated and treated samples were subjected to SDS/PAGE and Western blotting with an α-syn antibody. (*D*) PE content in WT cells expressing α-syn (2% [wt/vol] Gal). Total lipids were chemically extracted from each strain and analyzed using TLC. Values are means ± SD ($n = 3$). $^{*}P < 0.011$ and $^{**}P < 0.008$ were determined using one-way ANOVA with Dunnet post hoc test.

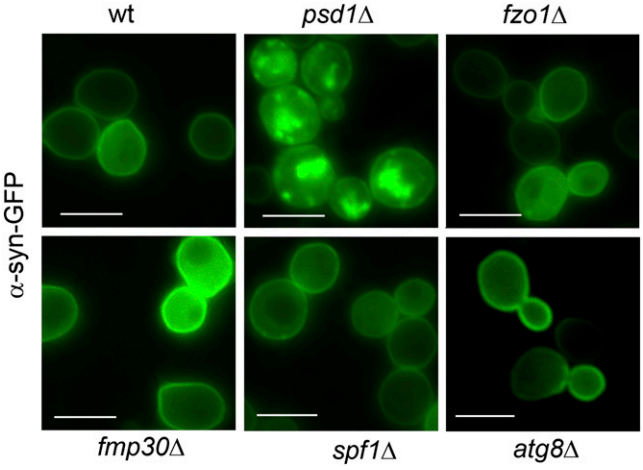

Fig. S6. α-syn does not form foci in *spf1*Δ or selected mutants. *SPF1* encodes for a P-type ATPase that regulates Ca^{+2} homeostasis in the ER. The indicated mutants harboring pAG426–α-syn–GFP were induced to express α-syn–GFP in the mixed medium, and the GFP fluorescence images were acquired after 5 h of induction.

Table S1. Yeast strains and plasmids

Strain	Genotype	Source
Wild type	BY4741; MATa his3-1 leu2-0 met15-0 ura3-0	Open Biosystems
*psd1*Δ	BY4741; *psd1::kanMX6*	Open Biosystems
*cho1*Δ	BY4741; *cho1::kanMX6*	Open Biosystems
*cho2*Δ	BY4741; *cho2::kanMX6*	Open Biosystems
*ino2*Δ	BY4741; *ino2::kanMX6*	Open Biosystems
*opi3*Δ	BY4741; *opi3::kanMX6*	Open Biosystems
*fzo1*Δ	BY4741; *fzo1::kanMX6*	Open Biosystems
*fmp30*Δ	BY4741; *fmp30::kanMX6*	Open Biosystems
*atg8*Δ	BY4741; *atg8::kanMX6*	Open Biosystems
*spf1*Δ	BY4741; *spf1::kanMX6*	Open Biosystems
*psd1*Δ–*ERG6*–*RFP*	*psd1*Δ;*erg6::ERG6*–mCherry–*SpHIS5*	This study
*psd1*Δ–*PEX6*–*RFP*	*psd1*Δ;*pex3::PEX3*–mCherry–*SpHIS5*	This study
Plasmid	Description	Source
pAG426GAL	2 μ, URA3, P_{GAL1}	Addgene
pAG425GAL	2 μ, LEU2, P_{GAL1}	Addgene
pRS315	*CEN* plasmid, LEU2	Kelly Tatchell
pAG426–α-syn	pAG426GAL, P_{GAL1}–α-syn	(14)
pAG425–α-syn	pAG425GAL, P_{GAL1}–α-syn	(12)
pAG426–α-syn–GFP	pAG426GAL, P_{GAL1}–α-syn–GFP	This study
pAG426–α-syn–RFP	pAG426GAL, P_{GAL1}–α-syn–RFP	This study
pMCZ-Y	UPRE–CYC1–LacZ on 2 μ plasmid	David J. Eide
pRS315–Fur4–EGFP	pRS315, P_{GAL1}–Fur4–EGFP	This study
YIPlac204TKC–DsRed–Express2–HDEL	DsRed with ER localization signal HDEL	Addgene
pRS315–preKar2–DsRed–Express2–HDEL	pRS315 inserted with DsRed–HDEL	This study
pRS416–Dlp2–GFP	pRS416, P_{DLD2}–GFP	Zhengchang Liu